

# First results of cruise S19 (PRIMAR Project): petrological and structural investigations of the Vema transverse Ridge (equatorial Atlantic)

Paola Fabretti<sup>1</sup>, Enrico Bonatti<sup>1</sup>, Alexander Peyve<sup>2</sup>,  
Daniele Brunelli<sup>1</sup>, Anna Cipriani<sup>1</sup>, Xenia Dobrolubova<sup>2</sup>,  
Vladimir Efimov<sup>2</sup>, Sergej Erofeev<sup>2</sup>, Luca Gasperini<sup>1</sup>,  
Jean H. Hanley<sup>1</sup>, Marco Ligi<sup>1</sup>, Andrey Perfiliev<sup>2</sup>,  
Vladimir Rastorguyev<sup>2</sup>, Yuri Raznitsin<sup>2</sup>, Galina Savelieva<sup>2</sup>,  
Victor Semjonov<sup>2</sup>, Sergei Sokolov<sup>2</sup>, Sergey Skolotnev<sup>2</sup>,  
Sara Susini, Ilya Vikentyev<sup>2</sup>

<sup>1</sup> ISMAR-CNR, Bologna

<sup>2</sup> GIN, Academy of Sciences, Moscow

Received: March 2010 / Accepted: May 2010 - PDF FOR PRINT

## SUMMARY

We carried out in January-March 1998 a geological-geophysical cruise to the Vema Fracture zone that offsets by 320 km the Mid Atlantic Ridge in the central Atlantic. This expedition (S19) was part of PRIMAR (Russian-Italian Mid Atlantic Ridge Project). The field work aimed at obtaining geophysical and petrological data from a prominent transverse ridge that runs on the southern side of the transform valley and constitutes a major topographic anomaly relative to the depth/square root of age relationship. Previous work had shown that a relatively undisturbed section of oceanic lithosphere is exposed on the northern side of the transverse ridge for roughly 270 km along a seafloor spreading flow line. Given an average spreading half rate of 16 mm/y, this length corresponds to over 16 My. One of the objectives of our expedition was to sample at close-spaced ( $\sim 5$  km) horizontal intervals the mantle ultramafic basal unit, in order to detect temporal variations of mantle composition and of accretion processes at ridge axis. Preliminary observations on ultramafic rock samples obtained at 35 sites suggest strong temporal variations of mantle structure and composition. Multichannel seismic reflection profiles were carried out in order to understand the processes that uplifted the transverse ridge and exposed the sliver of oceanic lithosphere. Magnetometric profiles were made to better constrain spreading rates.

**Key words:** Cruise S19 Report – Vema Ridge – Equatorial Atlantic

## 1 INTRODUCTION

The Vema Fracture Zone (VFZ) is the northernmost of a set of major transform faults that dis-

place the Mid Atlantic Ridge (MAR) in the equatorial region (Fig. 1). These fracture zones are characterized by long offsets, slow slip rates and

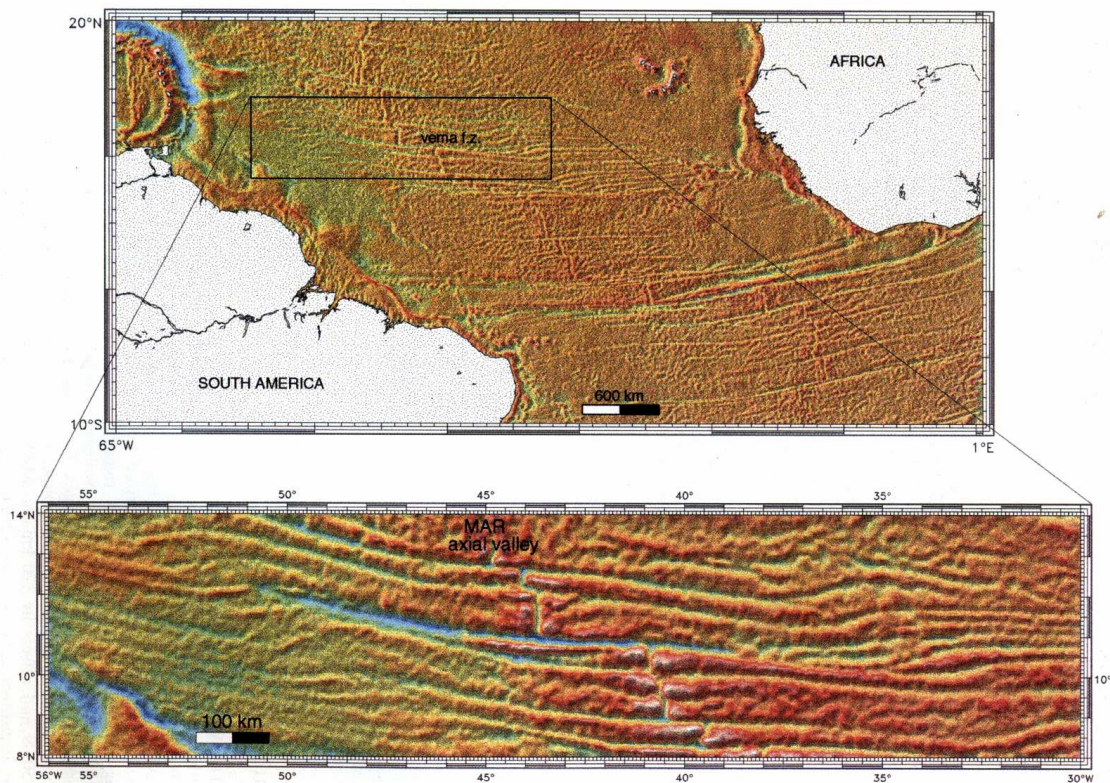


Fig. 1 - Free air satellite gravity anomaly map (Sandwell and Smith, 1997) of the Central Atlantic Ocean and Vema fracture zone.

Figure 1.

rough bathymetry, with deep transform valleys flanked by prominent transverse ridges. The Vema VFZ is located at a latitude of 10:50' N and offsets by 320 km the MAR. The transform valley, 15 to 22 km wide, trends mostly E-W and displays a flat floor on the north-facing wall of the VTR at longitude of 42:42' W, (Auzende et al. 1989).

This section includes from bottom to top: 1) upper mantle peridotites (~ 1km thick), 2) lower crustal gabbros (~ 500m thick), 3) sheeted dike complex (~1 km thick), and 4) upper basalt layer (200-800 m thick). Geophysical experiments (Robb & Kane 1975; Ludwig & Rabinowitz 1980; Loudon et al. 1986; Potts et al. 1986) and morphobathymetric data (Kastens et al. 1998) suggest that the exposed sliver of oceanic lithosphere extends continuously on the VTR for over 270 km along a seafloor spreading flow-line. Assuming an average half spreading rate of 16 mm/y for the last 30 My (Cande et al. 1988) this uplifted section corresponds to over 16.8 My. Therefore, the VTR gives us the opportunity to explore temporal variations of processes of accretion of the oceanic lithosphere such as composition, thermal properties and processes of melt extraction and injection in a slow spreading ridge. Determining temporal variations of ridge activity, as recorded in the structure and composition of the upper man-

tle rocks of different ages, was the main target of cruise S19. Accordingly, we carried out close-spaced rock sampling along the base of the VTR north-facing wall, where ultramafic rocks were expected. We also carried out seismic reflection profiles in order to detect variations of the thickness of the basaltic layer. These variations might be related to alternating cycles of magmatic and amagmatic accretion at the MAR. Seismic reflection profiles were collected to analyze transform-related tectonic deformations across the principal displacement zone of the Vema transform valley. We also obtained magnetometric data in order to determine spreading rates and ages of the oceanic crust along the Vema FZ.

## 2 METHODS AND INSTRUMENTATION

### NAVIGATION AND POSITIONING SYSTEM

The ship's position was determined by means of a Trimble 4000AX GPS receiver, with an accuracy of  $\pm 25$  m. An integrated positioning system was employed during the cruise: the R/V Strakhov main navigation system, NAVOS, interfaced with

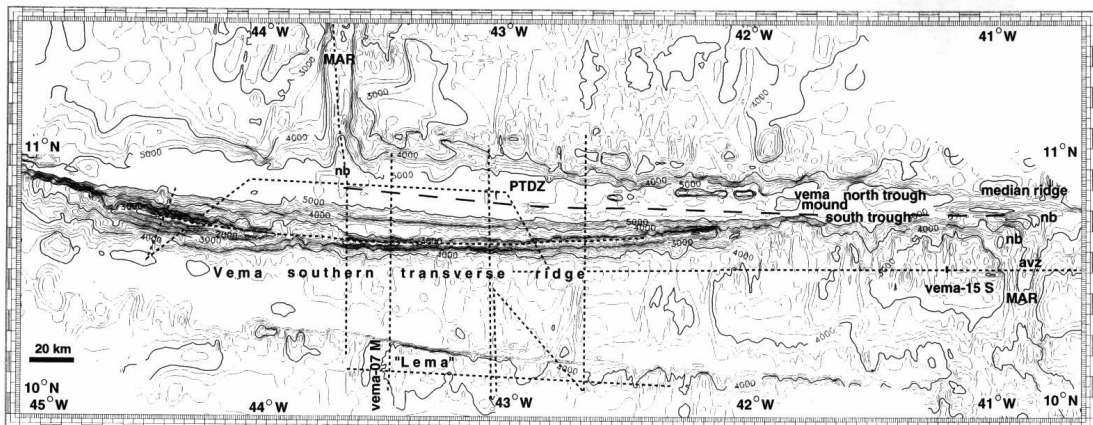


Fig. 2 - Contour map (each 200 m) of the Vema fracture zone bathymetry (data compiled from French and Italian surveys). The major morphostructural elements are indicated. MAR: Mid Atlantic Ridge; PTDZ: principal transform displacement zone; nb: nodal basin; avz: axial volcanic zone. Geophysical profiles Vema-15 S and Vema-07M discussed in the text are indicated. Dashed lines indicate seismic reflection profiles acquired during S19 and previous cruises of the PRIMAR project.

Figure 2. .

GPS, gyro and echo doppler, during the petrological sampling, in conjunction with a multibeam echosounder.

#### Multibeam morphobathymetry

Although the investigated area was, for the most part, already covered by multibeam data, we employed the on-board multibeam system to fill the gaps and to drive dredging operations. The multibeam system installed on the R/V Strakhov is an HOLLMING ECHOS 625, consisting of 15 (12.5 kHz) beams covering a swath of seafloor roughly 2/3 of the water depth in width. Multibeam data obtained during LDEO cruise EW93U5 (Kastens et al. 1998) with a Hydrosweep (Atlas-Krupp) system, were filtered and processed at IGM-CNR. The resulting detailed morphobathymetric maps of the Vema area were used during cruise S19.

#### Dredging

Dredging was performed by standard methods with a 10 tons hydraulic winch and steel wire, 17 to 12 mm in diameter. Dredges were made of iron barrels 2 cm thick, 70 cm in diameter and 1.4 m in length.

#### Multi-and single channel seismic reflection

Multichannel seismic reflection data were obtained using as seismic source an array of two G.I. guns (Sodera) towed at a depth of 6 m. Each gun has a capacity of 105 in<sup>3</sup> for the generator chamber, as well as for the injector; they operated at a pressure of 2000-3000 PS1 in harmonic mode. The receiving streamer (Teledyne) employed 24 channels

(with 20 hydrophones each), spaced 25 m apart. The nearest channel was located 150 m from the seismic source. The distance between shots was 50 m, allowing a coverage of 600%. Positioning and gun synchronization for each shot station was activated by the navigation software, NAVMAP, connected to GI gun controller system (Masini & Ligi 1995). Single channel lines were run at a speed of 7-8 knots using as seismic source a modified Bolt air gun and a high speed, towing single channel streamer designed by the Russian geophysical team of GIN (Moscow).

#### Magnetic

The Vema FZ is located close to the magnetic equator, causing the magnetic anomalies to be very weak relative to ambient noise. Corrections for diurnal variations are important in this area because they reach the same order of magnitude as the seafloor anomalies. We deployed one magnetometer based on the Overhauser effect, at a distance of 230 m from the GPS antenna. All magnetic profiles are located south of the Vema transform in the S.American plate. The data sampling was performed at rate of 6 sec by the navigation system.

The initial processing of magnetic data showed that the use of a single transducer configuration did not hamper the usefulness of the data. Fig. 5 shows part of magnetic profile VEMA-15 S, low-cut filtered (wavelength  $\geq 6$  hours, as an attempt to correct diurnal variations), after IGRF-95 removal, compared with its synthetic profile obtained by forward modeling based on Cande & Kent (1995) time scale, assuming 1 km magnetized layer. We note a general agreement between the two curves for a spreading rate at 15.5 mm/y, averaged over the last 5 Ma.

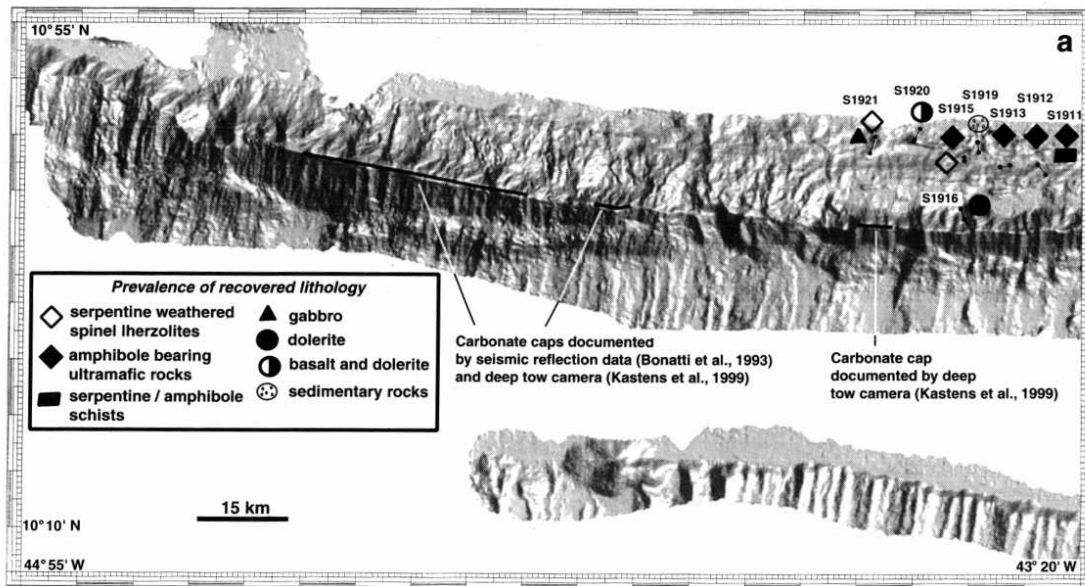


Fig. 3 - Shaded relief map of the Vema transverse ridge (VTR) multibeam bathymetry (illumination from 70°). These data, acquired by an Hydrosweep multibeam system during cruise EW9305, are gridded here at 100m steps. Location of the dredging sites during cruise S-19 are indicated. **a**, VTR western sector; **b**, VTR eastern sector and location of Nautilite profiles in Fig. 4.

Figure 3. .

### 3 MAJOR STRUCTURAL ELEMENTS OF THE VEMA FRACTURE ZONE

The Vema FZ is a right-lateral slow-slipping transform fault which displace the North America and African plates at 32 mm/y full rate (Cande et al. 1988). The Vema offsets the MAR axis by 320 km (Fig. 1), causing a maximum lithospheric age contrast across the transform fault of about 20 My at the RTI. The transform fault is located in an approximately E-W trending transform valley. The valley is 25-40 km wide as defined by the crests of the northern and southern walls, while the valley floor (defined by 5000 m contour) is 15-20 km wide (Fig. 2). The transform valley floor is covered by up to 1.5 km thick turbidites transported from the Amazon cone (Bader et al. 1970; Perch-Nielsen et al. 1977). The transform valley is bounded by 2-4 km high E-W walls. The southern wall is also the northern side of a major transverse ridge (VTR) (Fig. 2) more than 270 km long and up to 4.5 km high relative to the valley floor.

Seismic reflection data give evidence of a narrow ( $\approx$  2 km wide) zone of deformation in the turbidite deposits of the transform valley (Eittreim & Ewing 1975; Kastens et al. 1986). The disturbed zone has been interpreted as the active trace of the transform fault, or a principal transform displacement zone (PTDZ) (Fig. 2).

The transform valley, near the eastern RTI is divided into a northern and a southern trough by a median ridge (Fig. 2), which rises up to 1200

m above the valley floor. Seismic data show no active tectonics in the northern trough, but give evidence of at least 800m of undisturbed layered sediments, probably turbidites (Macdonald et al. 1986). In contrast, the southern trough is tectonically active, relatively free of sediment (less than 2 m) and covered by pillow basalt and sheet flow (Macdonald et al. 1986). Moving west the median ridge becomes buried by sediments; however, between 41:55'W and 41:45'W, it sticks out above the sediments by about 500m (Vema mound) (Fig. 2). It is approximately 8 km wide and 18 km long. There is no evidence that the Vema mound has undergone recent vertical tectonics. The northern side of the Vema mound was dredged and the following lithologies were recovered: gabbros and metagabbros 55%; serpentinized peridotites 25%; volcanoclastic 15%; basalt 5% (E. Bonatti, unpublished data).

At the Vema eastern RTI the MAR axial valley is covered by fresh and glassy pillow lavas (Macdonald et al. 1986). The axial neovolcanic zone extends into the nodal basin splitting it in two smaller subsidiary basins (Fig. 2). Two other fossil neovolcanic zones lie east and west of the nodal basin; they have a sediment cover (10-20 cm) and abundant fresh talus on their flanks, indicating that their constructional morphology has been affected by fault activity and mass wasting (Macdonald et al. 1986). Submersible observations

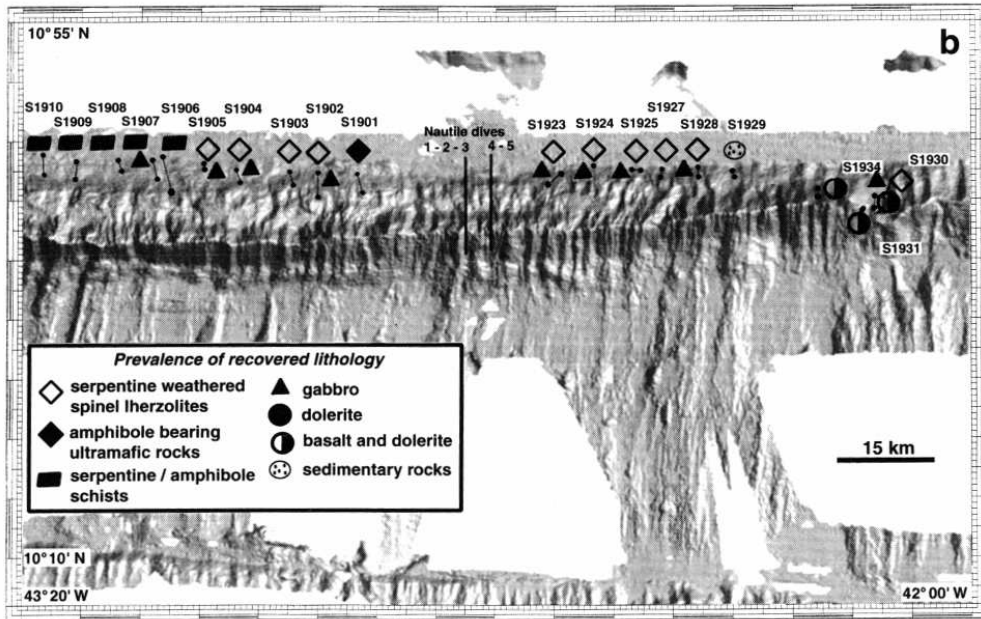


Figure 4 .

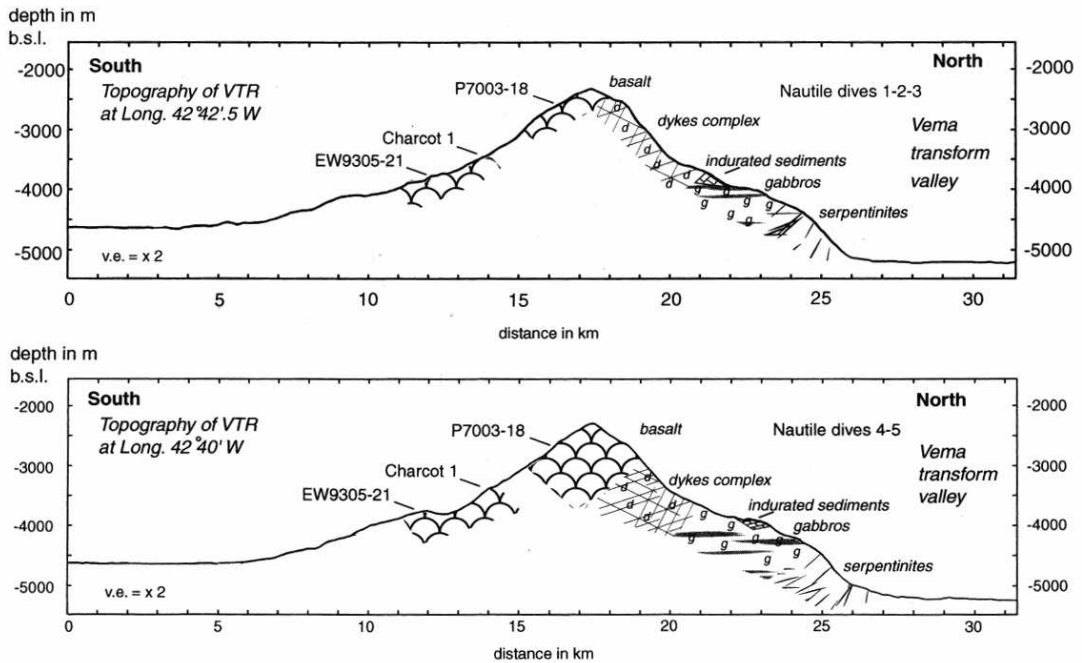


Fig. 4 - Topographic profiles of the VTR in correspondence of the Nautilite dives (Auzende *et al.*, 1989). For location see Fig. 3b. Rock samplings from previous cruises are indicated.

Figure 5 .

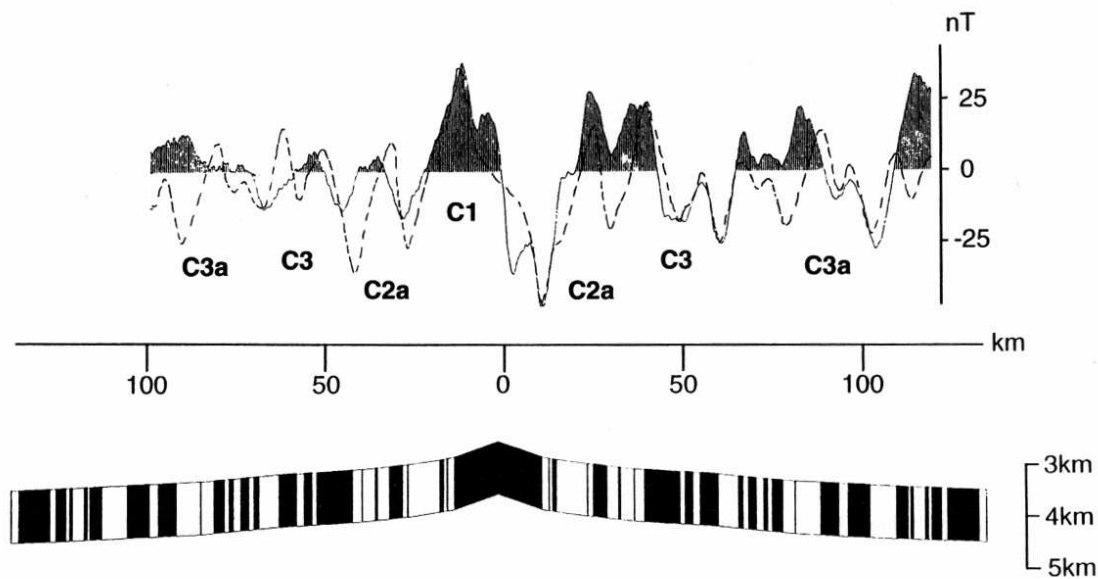


Fig. 5 - **a**, solid line: observed magnetic anomaly profile of Vema-15S (located in Fig. 2); dashed line: synthetic magnetic anomaly profile based on Cande and Kent (1995) time scale; **b**, 2D geological model assuming an oceanic magnetized layer 1 km thick and variable spreading rates. The best fitting between observed and synthetic anomalies is obtained with the following spreading rates: 15.5 mm/y (from 0 to 0.9 Ma, Chron 1) and 14.5 mm/y (from 0.9 to 1.7 Ma, Chron 1); 16.0 mm/y (from 1.7 to 2.5 Ma, Chron 2); 21.5 mm/y (from 2.5 to 3.5 Ma, Chron 2A); 12.0 mm/y (from 3.5 to 5.3 Ma, Chron 3).

Figure 6. .

confirm that nodal deep is sediment-free and covered by fresh pillow basalt flows.

Morphology and lithology of the southern Vema transverse ridge. The multibeam bathymetry, acquired by the R/V Ewing during cruise EW9305 LDEO (Kastens et al. 1998), gives a detailed image of the VTR morphology (Fig. 3a and b). The VTR develops 140 km west of the RTI. Ocean floor morphology between the VTR and the eastern RTI is characterized by abyssal hills, which rise, bending few hundred meters, toward the fracture zone. The VTR abruptly shoals from 3400 m to 2000 m below sea level through a sharp N-S wall, probably fault controlled. The VTR extends for over 270 km that correspond to 16.8 My (from 6.8 Ma to 23.6 Ma) assuming an averaged half spreading rate of 16 mm/y (Cande et al. 1988).

The morphology of the VTR is not homogeneous (Fig. 3a and b). N-S cross sections are mostly asymmetric, with a steeper northern side and a gentler southern side; however, some portions of the VTR are nearly symmetric. The northern side shows generally a bench or terrace along the middle part of the scarp. The upper slope of the VTR is cut by gullies and canyons and is steeper ( $>20^\circ$ ) than the lower slope ( $<2^\circ$ ). Fan shaped deposits, probably resulting from mass wasting and gravitational instability are observed at the base of both

the northern and southern slopes, particularly on the western, presumably older part of the VTR.

The western end of the VTR (Fig. 3a) has the shallowest summit, cresting at 450 m below sea level. Here the transverse ridge is capped by a  $\sim 500$  m thick shallow water limestone platform (Bonatti et al. 1983; ?; ?; Kastens et al. 1998). To the east ( $\sim 100$  km) another  $\sim 80$  m thick carbonate platform has been found on the VTR crest between 1000-1200 m below sea level (Fig. 3a) (?Kastens et al. 1998).

Rocks dredged from the VTR include samples from all the lithologies that characterize major units of the oceanic crust (Bonatti & Honnorez 1971; Melson & Thompson 1971; Bonatti & Honnorez 1976; Honnorez et al. 1984). Nevertheless, the stratigraphic relationships among the different units exposed on the northern side of the VTR were determined only after direct observation and sampling with the Nautilus submersible (Auzende et al. 1989). Two dive transects (Fig. 4), 5 km apart, located around 42:41' W, revealed the exposure of a complete sequence of oceanic lithosphere, consisting from bottom to top: mantle derived ultramafics, gabbros, dyke complex, basaltic upper crust.

*Mantle derived ultramafics*: serpentinized peridotites (1 km in thickness). The outcrops are massive or in part tectonically disrupted and

brecciated. Most of the rocks have porphyroclastic texture, some are mylonitic. Peridotites are highly serpentinized but contain relicts of olivine, orthopyroxene, clinopyroxene and spine], suggesting P-T equilibration under spine] peridotite facies. Some samples contain amphiboles (Cannat & Seyler 1995).

*Gabbros*: are generally massive and predominantly Fe- and Ti- rich, Their thickness is about 500 m.

*Dyke complex*: it outcrops almost continuously for a thickness of 700-1100 m, interrupted only by a few sub-horizontal or chaotic lava flows. The dykes are vertical and they are oriented parallel to the strike of the present MAR axis.

*Basaltic upper crust*: it consists of brecciated rather altered basalt (thickness of up to 800m).

One the objectives of cruise S19 was to sample at close horizontal intervals the lower, ultramafic unit exposed on the northern side of the VFR, as described in the next section.

### 3.1 Rock sampling during cruise S19: lateral variation of the ultramafic rocks composition

From the lower part of the northern scarp of the VTR thirty five dredge stations were carried out. They were spaced about 3 nautical miles apart along a sea floor spreading flow line, with the main goal of recording temporal variations in upper mantle composition. Sampling was done both west and east of the Nautil sections, i.e., west of 42:50'W and east of 42:30'W (Fig. 3a and b).

The western area include a set of 22 dredge stations, located between 43:35'W and 42:52'W, a stretch of 87 km equivalent to a time interval of 3.9 My (from Cande & Kent (1995) time scale).

The eastern area included a set of 13 dredge stations, carried out between 42:36' W and 42:08' W, a stretch of 55 km corresponding to 2.5 My (from Cande & Kent (1995) time scale).

A shipboard description of the dredge hauls is reported in Tab. 1.

Serpentinized peridotites are the main rock type recovered at all sites deeper than 4000 m. They make up about 60% (by weight) of the total material recovered from all sites. Other common lithotypes are gabbros (10%), dolerites (10%), basalts (5%), limestones and breccias (15%). FE-Mn films and crusts often cover the different lithotypes.

A preliminary description of the samples suggests systematic lateral variations in the structure and composition of the ultramafic unit exposed on the VTR. Some domains of the VTR basal unit are dominated by relatively undeformed porphyroclastic peridotites. In the other domains strongly deformed, mylonitic peridotites prevail, frequently containing amphiboles. These different domains reflect probably different processes

of lithosphere emplacement ("magmatic" accretion versus "amagmatic" extension) at ridge axis at different times. In addition preliminary electron probe analysis of mantle equilibrated relict minerals (olivine, opx, cpx, and spinel) suggest variations in composition that may reflect variable degrees of depletion.

These preliminary data confirm our assumptions that the VTR will release important information on the temporal variations of processes of formation of the oceanic lithosphere at the axis of the Mid Atlantic Ridge. Analytical work is in progress with the aim of achieving this task.

### 3.2 Seismic reflection profiles acquired in S19 cruise: the image of VTR and PTDZ tectonics

Four N-S seismic reflection profiles were acquired across the Vema transform to investigate the structural style of the VTR and PTDZ (Fig. 2). Our seismic lines were extended to a roughly E-W oriented scarp, which runs 65 km south of the Vema transform. This structure named ("Lema" FZ (Kastens et al. 1998) is markedly asymmetric and probably marks a former transform plate boundary. We will describe the major features observed along one of these seismic sections (Vema-07M, for location see Fig. 2) that runs S-N within the S. American plate, from the Lema FZ to the Vema transform valley. A seismic image of Lema FZ is visible between shot 200 and shot 750 (Fig. 6a): the north-facing flank bounds a small sedimentary basin. The basin infilling appears to be undisturbed, and onlapping the fault scarp and the oceanic crust. The sea floor to the south of this structure (the hanging-wall) lies about 1000 m above the oceanic crust on the northern side (foot-wall). Moving northward (from shot 800 to shot 1300, Fig. 6b) a series of mounds are present. They may represent sedimentary deposits derived from slope instability along the southern wall of VTR. The complex geometry of the reflections, the chaotic seismic facies and scoop-shaped reflectors suggest that slumpings and/or mega-slumpings may have occurred on the southern wall of VTR. The VTR rises between shot 1300 and 1750 (Fig. 6c) reaching here a minimum depth of about 1500 m below the sea level. The northern flank is terraced with a major slope break at shot 1590. The seismic profile shows, between shots 1410 and 1490, a southward dipping reflector; it could represent the base of basaltic layer 2a. The middle scarp terrace represents the top of the gabbro sequence (Auzende et al. 1989). Rugged topography is present at the base of VTR slope, suggesting active phenomena of gravity instability along low angle detachment surfaces. These deposits pass laterally to the Vema valley sedimentary sequence, between shot 1850 and shot 2250 (Fig. 6d). The transform valley infilling shows fine layering, al-

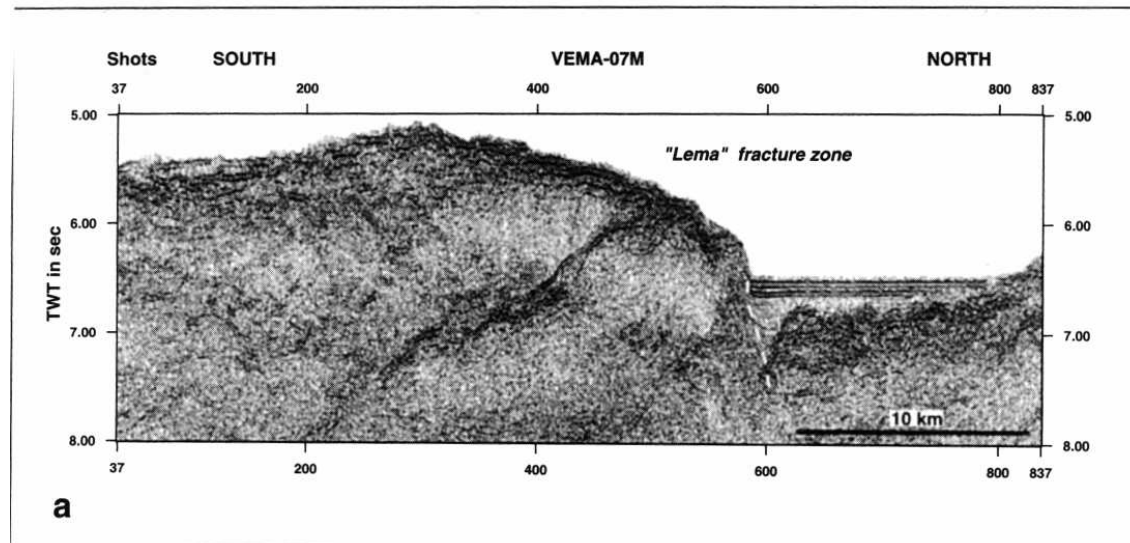


Figure 7. .

ternated by regularly spaced stronger reflectors, Tectonic deformation is concentrated in a 4 km wide sector at the transform valley center (Fig. 6d) where the PTDZ is located. Here evidence of compressive deformations can be observed throughout the sediment column down to the valley basement. The median ridge is visible buried below 0.5 sec of sediments.

#### 4 CONCLUSIONS

- 1 The presence of a prominent transverse ridge is typical of several fracture zone ( i.e., Romanche FZ, Kane FZ, etc.). A number of factors may have contributed to their formation. These factors, as discussed in details by several authors (Bonatti 1978; Bonatti & Crane 1982; Parmentier & Haxby 1986; Rutter & Brodie 1987; Chen 1988; Morgan & Forsyth 1988; Bonatti et al. 1994; Pockalny et al. 1996), include thermal rejuvenation of old lithosphere near the RTI, frictional shear heating along the transform, lithospheric flexure due to thermal stresses, nonlinear viscoelastic deformation of the lithosphere, hydration/dehydration reaction of upper mantle rocks near the transform igneous activity and transform-related transpression transtension. Compressional or extensional stresses, due to reorientation of the transform fault and ridge axis following changes in the direction of the plate motions, are able to build up corrugation or flexural uplifted blocks, respectively, with vertical motions comparable to those observed in transverse ridges
- 2 The Vema transverse ridge is unique in so far as it exposes a nearly undisturbed and complete section of oceanic lithosphere with lateral con-

tinuity, it gives us the opportunity to study the signature of temporal and spatial variations in the activity of a slow spreading ridge such as MAR. Following this main objective we sampled ultramafic rocks, at sites 5 km apart, along a 143 km long stretch of VTR northern wall, in a depth range of 4300-5000 m. The VTR can be interpreted as a continuous sector of oceanic lithosphere, but characterized by sub-domains coherent in lithology. Preliminary observations on these samples show systematic lateral variations in the structure and composition of the upper mantle, caused probably by temporal variations in the processes of accretion at ridge axis. Some intervals are made prevalently by coarse-grained, porphyroclastic peridotites, while in other intervals strongly deformed, mylonitic peridotites are prevalent. In addition, amphibole-rich ultramafics are common in some intervals.

- 3 Slide and slumping deposits are visible at the base of the southern scarp of the VTR (Fig. 6). Slope instability probably contributes, in this area, to the symmetric profile of the VTR. The seismic reflection data reveal the presence of two listric slide planes at the base of the northern wall of VTR. The origin of the mid-scarp terrace on the northern side of the VTR is probably related to selective erosion between massive or slightly tectonized gabbros and the dyke complex. There is no evidence of tectonic control on the terrace.
- 4 The PTDZ has been subjected to recent compressional movements.
- 5 The sedimentary rocks sampled along the lower VTR scarp are mostly products of the physical and chemical disgregation of the transverse ridge rock units. The upper VTR slope (Fig



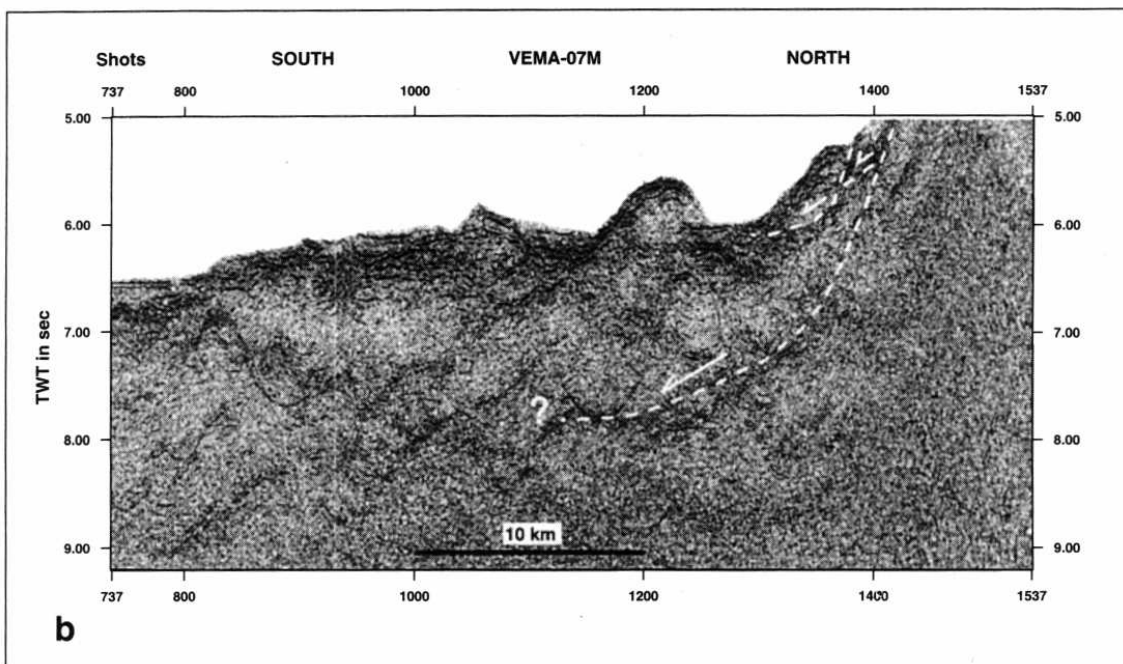


Figure 8. .

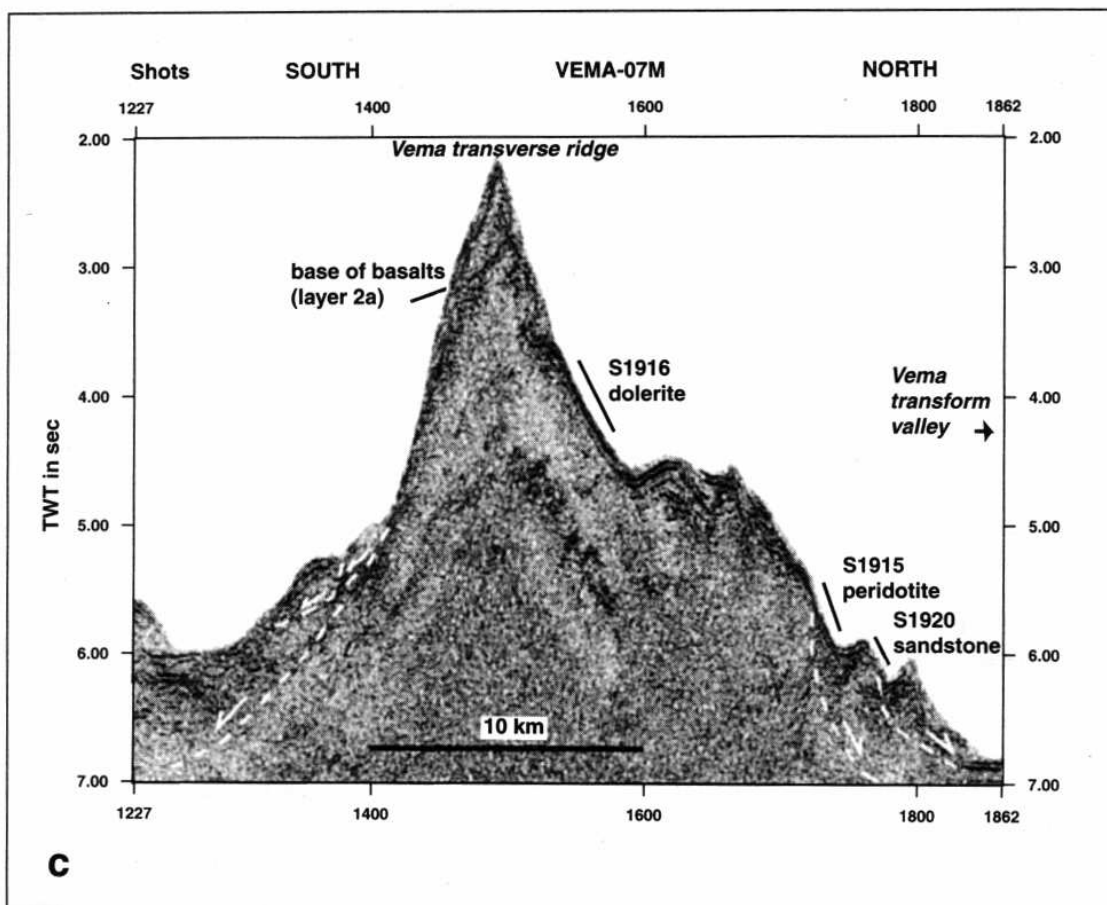


Figure 9. .

Fig. 6 - Vema-07M time migrated section. The on-board processing performed on the section includes: -trace editing (noise and missing shots); - gap deconvolution (gap 24 msec, operator length 55msec); -sorting of CDP gathers; -brute stacking; -velocity analysis; -NMO correction; -band pass filtering; -stacking; -time migration. **a**, time migrated section of «Lema» fracture zone; **b**, time migrated section of chaotic facies at the base of the VTR southern flank; **c**, time migrated section of Vema transverse ridge. The dredged lithologies are reported; **d**, time migrated section of Vema transform valley.

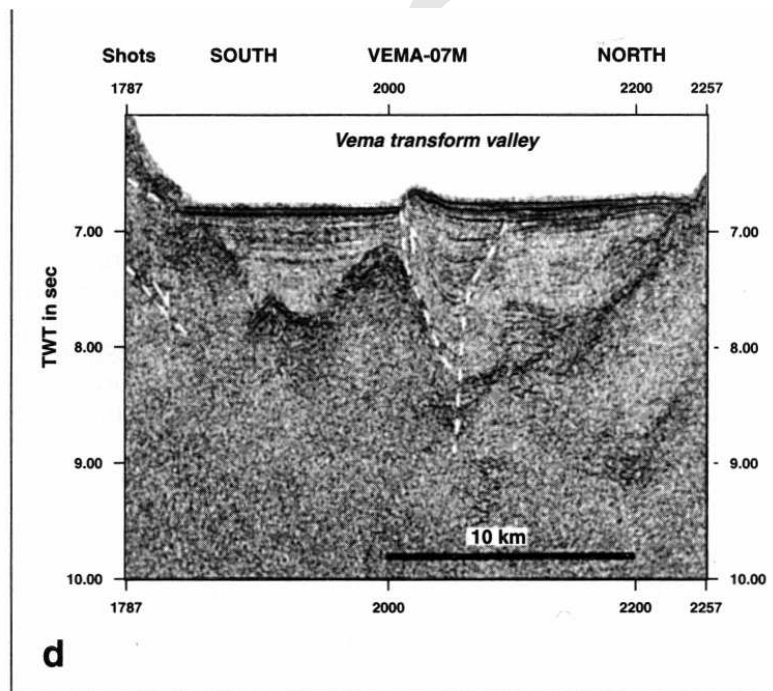


Figure 10. .

3a e 3b) is a typical young active slope ( $>20^\circ$ ) where intense mass wasting has occurred. It is cut by scoop-shaped scarps leading to a distinct gully and canyon topography. These gullies and canyons cut into the basalt and dyke complex unit, channeling debris transport downslope toward a gentler slope ( $<20^\circ$ ). At the base of these slopes or where the terrace is present, the gully and canyon network leads to coalescing debris fans. The sedimentary samples that we collected at various locations along the VTR include sedimentary breccias, sandstones and limestones: their matrix is rich of pelagic components such as foraminifera that will allow age determinations.

We are very grateful to the Captain Leonid Sazonov, to the officers and crew of the R/V A.N. Strakhov for their skill and cooperation in the field work. We are also grateful to P.Dall'Olio, G.Gallerani, V. Landuzzi, V.Landuzzi, M.Marani and M.Mengoli, who in various capacities helped make the field work possible. Contribution N. 1154 of the Istituto per la Geologia Marina del CNR.

## REFERENCES

- Auzende, J.-M., Bideau, D., Bonatti, E., Cannat, M., Honnorez, J., Lagabriele, Y., Malavieille, J., Mamaloukas-Frangoulis, V., & Mevel, C., 1989. Direct observation of a section through slow-spreading oceanic crust, *Nature*, **337**.
- Bader, R. G., Gerard, R. D., Benson, W. E., Bolli, H. M., Hay, W. W., Rothwell, W. T., Ruef, M. H., Riedel, W. R., & Sayles, F. L., 1970. Introduction, *Deep Sea Drilling Project, Initial Reports*, **4**, 59-67.
- Bonatti, E., 1978. Vertical tectonism in oceanic fracture zones, *Earth Planet. SC. Lett.*, **37**, 369-379.
- Bonatti, E. & Crane, K., 1982. Oscillatory spreading explanation of anomalously uplifted crust near oceanic transform, *Nature*, **300**, 343-345.
- Bonatti, E. & Honnorez, J., 1971. Non spreading crustal blocks at the Mid-Atlantic Ridge, *Science*, **174**, 1329-1331.
- Bonatti, E. & Honnorez, J., 1976. Sections of the earth's crust in the Equatorial Atlantic, *J. Geophys. Res.*, **81**, 4114-4117.
- Bonatti, E., Sartori, R., & Boersma, A., 1983. Vertical crustal movements at the Vema fracture zone in the Atlantic: evidence from dredged limestone, *Tectonophysics*, **91**, 213-232.
- Bonatti, E., Ligi, M., Gasperini, L., Peyve, A., Ravnitzin, Y., & Chen, Y. J., 1994. Transform migration and vertical tectonics at the Romanche Fracture Zone, equatorial Atlantic, *J. Geophys. Res.*, **99**, 21779-21802.
- Cande, S. C. & Kent, D., 1995. Revised calibration of the geomagnetic polarity time scale for the Late Cretaceous and Cenozoic, *J. Geophys. Res.*, **100**, 6093-6095.
- Cande, S. C., LaBrecque, J. L., & Haxby, W. F., 1988. Plate kinematics of the South Atlantic: chron C34 to the present, *J. Geophys. Res.*, **93**, 13479-13492.
- Cannat, M. & Seyler, M., 1995. Transform tectonics, metamorphic plagioclase and amphibolite-

- zation in ultramafic rocks of the Vema transform fault (Atlantic Ocean), *Earth Planet. Sci. Lett.*, **133**(3-4), 283–298.
- Chen, Y., 1988. Thermal model of oceanic transform faults, *J. Geophys. Res.*, **93**, 8839–8851.
- Eittreim, S. & Ewing, M., 1975. Vema Fracture Zone transform fault, *Geology*, **3**, 555–558.
- Honnorez, J., Mvel, C., & Montigny, R., 1984. Geotectonic significance of gneissic amphibolites from the Vema fracture zone, equatorial Mid-Atlantic Ridge, *J. Geophys. Res.*, **89**(B13)(11), 37–11.
- Kastens, K., Bonatti, E., Caress, D., G., G. C., Dauteuil, O., Frueh-Green, G., Ligi, M., & Tartarotti, P., 1998. The Vema transverse ridge (Central Atlantic), *Marine Geophys. Res.*, **20**(6), 533–556.
- Kastens, K. A., Macdonald, K. C., Miller, S., & Fox, P. J., 1986. Deep Tow studies of the Vema Fracture Zone: II. Evidence for tectonism and bottom currents in the sediments of the transform valley floor, *J. Geophys. Res.*, **91**, 3355–3368.
- Louden, K. E., White, R. S., Potts, C. G., & Forsyth, D. W., 1986. Structure and seismotectonics of the Vema Fracture Zone, Atlantic Ocean, *J. Geol. Soc.*, **143**(5), 795–805.
- Ludwig, W. J. & Rabinowitz, P. D., 1980. Structure of Vema Fracture Zone, *Marine Geology*, **35**, 99–110.
- Macdonald, K. C., Fox, P. J., Miller, S. P., Kastens, K. A., & Castillo, D., 1986. Deep-tow studies of the Vema Fracture Zone: I. The tectonics of a major slow-slipping transform fault and its intersection with the Mid-Atlantic Ridge, *J. Geophys. Res.*, **91**, 3334–3354.
- Masini, L. & Ligi, M., 1995. Sistema di controllo e sincronizzazione cannoni sismici ad aria compressa, Tech. Rep. 37, IGM-CNR, Rapporto Tecnico.
- Melson, W. G. & Thompson, G., 1971. Petrology of a transform fault zone and adjacent ridge segments, *Phil. Trans. Royal Soc. Lond.*, **268**, 423–441.
- Morgan, J. P. & Forsyth, D. W., 1988. Three-dimensional flow and temperature perturbations due to a transform offset: Effects on oceanic crustal and upper mantle structure, *J. Geophys. Res.*, **93**, 2955–2966.
- Parmentier, E. M. & Haxby, W. F., 1986. Thermal stresses in the oceanic lithosphere: evidence from geoid anomalies at fracture zones, *J. Geophys. Res.*, **91**, 7193–7204.
- Perch-Nielsen, K., Supko, P., Boersma, A., Bonatti, E., Carlson, R., McCoy, F., Neprochnov, Y., & Zimmerman, H., 1977. Site 353: Vema Fracture Zone, *DSDP Reports*, **XXXIX**, with an additional report from D.E. Fisher.
- Pockalny, R., Gente, P., & Buck, W. R., 1996. Oceanic transverse ridges: a flexural response to fracture-zone-normal extension, *Geology*, **24**, 71–74.
- Potts, C. G., White, R. S., & Loudon, K. E., 1986. Crustal structure of Atlantic Fractures Zones. II - The Vema Fracture Zone and transverse ridge, *Geophys. J. R. Astron. Soc.*, **86**, 491–513.
- Robb, J. M. & Kane, M. F., 1975. Structure of the Vema Fracture Zone from Gravity and Magnetic Intensity Profiles, *J. Geophys. Res.*, **80**(32), 4441–4445.
- Rutter, E. H. & Brodie, K. H., 1987. On the mechanical properties of oceanic transform faults, *Ann. Tectonicae*, **1**, 87–96.